Estimation of Atmospheric Particulates and Dry Deposition Particulate-bound Mercury Hg(p) in Sha-Lu, Taiwan

Guor-Cheng Fang[*], I-Lin Yang, Chia-Kuan Liu

Department of Safety, Health and Environmental Engineering, HungKuang University, Sha-Lu, Taichung 433, Taiwan

ABSTRACT

Ambient air samples were collected between March 17, 2009 and May 22, 2009 at a highway traffic site located in Sha-Lu, central Taiwan. Atmospheric particulates and particulate bound mercury Hg(p) dry deposition fluxes, concentrations ($PM_{2.5}$, $PM_{2.5–10}$ and TSP) were studied. The results indicate that the average ambient air particles dry deposition, $PM_{2.5}$, $PM_{2.5–10}$ and TSP. concentrations were 145.03 $\mu g/m^2$-min and 15.47, 9.50, 65.14 $\mu g/m^3$, respectively. And the average dry deposition, $PM_{2.5}$, $PM_{2.5–10}$ and TSP bound mercury Hg(p) concentrations were 0.9519 ng/m^2-min and 0.1140, 0.0106, 0.0763 ng/m^3, respectively. In addition, the average ambient air particles bound mercury Hg(p) compositions for $PM_{2.5}$, $PM_{2.5–10}$ and TSP were 3.60, 3.45 and 44.99 ng/g, respectively. The results indicate that both of these two models (Baklanov and Sorensen, 2001; Zhang *et al*., 2001) are estimated as the measured dry deposition mass flux. The Baklanov model performs better results in the prediction of mass dry deposition flux. In addition, both of these two models slightly underestimate the measured dry deposition mass flux for particle bound Hg(p). Zhang's model performs better results in the prediction of Hg(p) dry deposition flux.

Keywords: Particle bound mercury; Dry deposition model; Baklanov and Sorensen's model; Zhang's model.

INTRODUCTION

In recent years, there has been an increase in human health and environmental concerns related to mercury emissions because of the toxicity of methylmercury. Methylmercury is commonly produced by methylation of inorganic mercury in aquatic environments and is subsequently bioaccumulated in fish through the food chain. The atmosphere is an important source of mercury for surface waters and terrestrial environments. Understanding the mercury emissions-to-deposition cycle is required for the assessment of the environmental risks posed by methylmercury (EPRI, 1996; Schroeder and Munthe, 1998; Sakata and Asakura, 2007).

These studies as well as studies conducted in other parts of the US have shown elevated Hg concentrations and deposition close to urban/industrial regions, with lower values in rural areas (Dvonch *et al*., 1998; USEPA, 1998; Liu *et al*., 2007). It is speculated that the spatial gradients of Hg deposition are largely caused by contributions of Hg emissions from urban/industrial regions, where concentrations of mercury species (Gaseous Eelemental Mercury (GEM),

Reactive Gaseous Mercury (RGM), and particulate mercury Hg(p)), particularly concentrations of RGM and Hg(p), are much higher and more variable than in rural areas. There have been only a few studies attempting to locate mercury sources using hybrid receptor models (Poissant, 1999; Lin *et al*., 2001), and none of them compared the results of different receptor models. This research was undertaken to identify the locations of mercury sources that affect New York State and to determine the contribution of in-state versus out-of-state sources, using several different hybrid receptor models (Han, 2007). Due to its high solubility and surface reactive properties, RGM can be removed from the atmosphere through both dry and wet deposition at rates much faster than GEM (Lin and Pehkonen, 1999; Liu *et al*., 2001). A large fraction of the Hg(p) is measured in the 2.5 mm size range which, in the absence of precipitation, has slower removal rates and longer resident times than RGM (Schroeder and Munthe, 1998; Liu *et al*., 2001) and has a much shorter residence time if a few hours to several days before departing the atmospheric cycle(Calvert and Lidberg, 2005). Essential processes in CAM (Gong *et al*., 2000; Zhang *et al*., 2001) include particle sources, transport and removal mechanisms. One of the removal processes is the particle dry deposition, which is a complex process depending on physical and chemical properties of the aerosol, the underlying surface characteristics and micro-meteorological conditions. Only a few direct measurements of mercury fluxes and speciation from natural sources are available in the literature (Gustin *et*

---
[*] Corresponding author. Tel.: (886)-4-26318652 ext 1110;
Fax: (886)-4-2631-0744
E-mail address: gcfang@sunrise.hk.edu.tw

al., 1999; Wallschlager *et al.*, 1999; Engle *et al.*, 2001; Engle and Gustin, 2002; Lindberg *et al.*, 2002; Zhang *et al.*, 2002).

The method/device used in this study is the same as those previous dry deposition related studies (Fang *et al.*, 2006). Knowledge of particle dry deposition is far from complete due to the complex dependence of deposition on particle size, density, terrain, vegetation, meteorological conditions and chemical species. A variety of dry deposition parameterizations have been used in large and regional-scale transport models, and are reported in a review by Ruijgrok *et al.* (1995). Numerous regional and global-scale modeling studies have been conducted to obtain a better understanding of the relationships between the sources, transport, transformation and fate of the important mercury species (Shannon and Voldner, 1995; Pai *et al.*, 1997; Bullock, 2000; Petersen *et al.*, 2001; Seigneur *et al.*, 2001; Bullock and Brehme, 2002; Ryaboshapko *et al*., 2002; Cohen *et al.*, 2004; Dastoor and Larocque, 2004; Travnikov, 2005; Gbor *et al.*, 2006).

The objective of this study was to: 1) measure the dry deposition concentrations of ambient air particles and particle bound mercury Hg(p) using the total suspended particulates (TSP) sampler, and dry deposition plate (DDP); 2) measure the average compare-bound mercury Hg(p) in $PM_{2.5}$, $PM_{2.5-10}$ and TSP; 3) bale the dry deposition fluxes of particles and particle bound mercury Hg(p) with dry deposition calculated and 4) compare the results of calculated dry deposition fluxes with various models to measured dry deposition fluxes for particles and particle bound mercury Hg(p).

DRY DEPOSITION MODEL

Baklanov and Sorensen's Model

Baklanov and Sorensen (2001) had proposed improved deposition models for long-range deposition computation. It is realized by defining the dry deposition velocity as the inverse of a sum of resistances r_a, r_b, r_c in three sequential layers (Wesely, 1989; Yamartino, 1989; Zanetti, 1990; Näslund and Thaning, 1991; Gustin *et al.*, 1999; Poissant, 1999; Wallschlager *et al.*, 1999; Lin *et al.*, 2001; Calvert and Lidberg, 2005; Fang *et al.*, 2006; Ghose and Majee, 2007; Basu *et al.*, 2009), in the following form for gaseous pollutants:

$$V_d = (r_a + r_b + r_c)^{-1}, \tag{1}$$

where r_a is the aerodynamic resistance, r_b is the resistance to penetration across the atmospheric laminar sublayer, and r_c is the resistance associated with direct pollutant-surface interaction.

For particles, Baklanov and Sorensen (2001) suggest that the transfer resistance, r_c, is negligible, since once the particle encounters the surface, it is considered to be deposited. For particles, Seinfield suggested another term, $r_a r_b v_g$, instead of r_c.

Additionally, this formula for the dry deposition velocity of particles has a term, defined by the sedimentation/ gravitational settling of particles:

$$V_d = (r_a + r_b + r_a r_b v_g)^{-1} + v_g, \tag{2}$$

where v_g is the gravitational settling velocity.

The aerodynamic resistance r_a depends on meteorological parameters, such as wind speed, atmospheric stability and surface roughness, and can be derived:

$$r_a = [\ln(Z_s/Z_o) - \Psi_c]/k u_*, \tag{3}$$

where Ψ_c is the stability function,

$$\Psi_c = -5Z/L \quad \text{for } Z/L > 0, \tag{4}$$
$$\Psi_c = \exp[0.598 + 0.390\ln(-Z/L) - 0.09(\ln(-Z/L))^2]$$
$$\text{for } Z/L < 0. \tag{5}$$

Here, L is the Monin-Obuhkov length, Z_s the height of the first reference level, Z_o the roughness height, k von Karman's constant ($k \doteq 0.4$), and u_* the friction velocity.

The surface layer resistance, r_b, depends on parameters characterizing diffusion across a laminar sublayer, i.e. on molecular rather than turbulent properties. Therefore, this parameter will be different for particles and gases. For particles, according to Zannetti (1990) the surface layer resistance can be expressed as a function of the Schmidt number, Sc = ν/D, and the Stokes number, St:

$$r_b = (S_c^{-2/3} + 10^{-3/St})^{-1} u_*^{-1} \tag{6}$$

where St = $V_g u_*^2/g\nu$, ν is the kinematic viscosity of air (1.5×10^{-5} m²/s), D is the Brownian diffusivity of a pollutant, D = $k_B TC/12\pi\mu r_p$, r_p the particle radius, C the Cunningham correction factor, T the temperature, k_B the Boltzmann constant, and μ the dynamic viscosity coefficient (1.8×10^{-5} kg/ms).

For particle diameters less than approximately 3.5 μm, for which the airflow around the falling particle can be considered laminar, the gravitational settling velocity v_g, is given by Stokes law (Hinds, 1982):

$$v_g = [2C(\rho_p - \rho)g r_p^2]/9\nu, \tag{7}$$

where ρ_p and ρ are the particle and air densities, g is the gravitational acceleration, is the particle radius, ν is the kinematic viscosity of air and C is the Cunningham correction factor (Yamartino, 1989).

However, for larger particles, Stokes law is not valid, and in the turbulent regime an iterative procedure to solve the equation for the terminal settling velocity will be used according to Näslund and Thaning (1991):

$$Dw_p/dt = (w - w_p)f(V) - \beta g, \tag{8}$$
$$f(V) = 3\rho VC_d/8r\rho_p, \tag{9}$$
$$V = ((u - u_p)^2 + (v - v_p)^2 + (w - w_p)^2)^{1/2}, \tag{10}$$
$$C_d = 24/Re[1 + 0.173(Re)^{0.657}] + 0.413/(1 + 16300(Re)^{-1.09}); \tag{11}$$

where V is the relative velocity of particles, u, v, w, u_p, v_p, w_p are the air and particle velocity components, β is the buoyancy effect parameter, $\beta = (\rho_p - \rho)/\rho_p$, C_d is the drag

coefficient for the static case , and Re is the Reynolds number, Re = 2Vr/ν.

20 μm average particle size in TSP was selected in this study to model the particle-bound mercury dry deposition fluxes (Ghose and Majee, 2007). Then calculated dry deposition velocities will be multiplied by the measured ambient air concentrations to obtain calculated dry deposition fluxes for ambient air and particle-bound mercury (Hg(p)). The calculated dry deposition fluxes will then be compared with the measured dry deposition fluxes. The results of the fluxes ratios for calculated/measured dry deposition were then used to evaluate weather the results over-or underestimate the dry deposition fluxes.

Zhang's Model

Zhang *et al*. (2001) have used the same approach as Slinn's (1982) model for particle dry deposition, but using simplified empirical parameterization for all deposition processes. The dry deposition velocity Vd can be expressed as

$$Vd = Vg + 1/(Ra + Rs), \tag{12}$$

where Vg is the gravitational settling velocity, Ra is the aerodynamic resistance above the canopy, Rs is the surface resistance.

The aerodynamic resistance is calculated as

$$Ra = [ln(ZR/Z0) - \Psi H]/ku_* \tag{13}$$

where ZR is the height at which the dry deposition velocity Vd is calculated, Z0 is the roughness length, ΨH is the strability function, *k* is the Von Karman constant and u* is the friction velocity. Rs depends on the collection efficiency of the surface and is determined by the various deposition processes, the size of the deposition particles, atmospheric conditions and surface properties. In their study (Zhang *et al*., 2001), Rs is parameterized as

$$Rs = 1/[\varepsilon 0\ u_*\ (EB + EIM + EIN)\ R1] \tag{14}$$

where EB, EIM, EIN are collection efficiency from Brownian diffusion, impaction and interception, respectively; R1 is the correction factor representing the fraction of particles that stick to the surface. ε0 is an empirical constant and is taken as 3 for all land use categories (LUC).

For Brownian diffusion, there is evidence that is a function of Schmidt number, Sc, given as

$$EB = Sc - \gamma \tag{15}$$

The Schmidt number is the ratio of the kinematic viscosity of air, ν, to the particle Brownian diffusivity, D (Sc = ν/D). γ usually lies between 1/2 and 2/3 with larger values for rougher surfaces.

The parameter governing impaction process is the Stokes number, St, which has the form St = Vg u*/gA for vegetated surfaces (Slinn, 1982) and St = Vg u*2/ν for smooth surfaces or surfaces with bluff roughness elements (Giorgi, 1988).

"A" is the characteristic radius of collectors.

Slinn (1982) used a semi-empirical fit for smooth surfaces, for which the collection efficiency by impaction is
Deciduous broadleaf trees

$$EIM = 10-3/St \tag{16}$$

Zhang *et al*. (2001) used the following simple form for calculating collection efficiency by interception:

$$EIN = 1/2(dp/A)2 \tag{17}$$

The characteristic radius "A" is given for different land use and seasonal categories.

Particles larger than 5 μm may rebound after hitting a surface. This process may be included by modifying the total collection efficiency by the factor of R1, which represents the fraction of particles sticking to the surfaces. Slinn (1982) suggested the following form for R1:

$$R1 = exp(-St1/2) \tag{18}$$

EXPERIMENTAL METHODS

Sampling Location

Ambient particles were collected on the roof of the Medical and Industrial Building at Hungkuang University in Taichung County, Taiwan (Fig. 1). The building is eight-stories tall (25 m) and located on the highest point (500 m) of Da Du Mountain. This sampling location is about 100 m away from a highway (Formosa Highway II) and about 10 km from the Taiwan Straits. Taichung Thermal Power Plant (TTPP) was developed on 281 hectares and located along the coast of the west side of sampling site. It is a coal combustion-based TTPP supplies about 4400 MW of electric power to meet the energy needs of central Taiwan. It was located about 10 km west of the Hungkuang University sampling site.

Meteorological conditions at the Hungkuang University site were determined using a Watchdog Weather Station Model 525 (Spectrum Technologies, Inc, USA). This weather station can provide data on wind speed, wind direction, temperature and humidity during the sampling period.

Sampling Program
PS-1 Sampler

The PS-1 sampler is a complete air sampling system designed to simultaneously collect total suspended airborne particles (Graseby-Andersen, GMW High Volume Air Sampler). The maximum particle size collected with the PS-1 sampler is 100 μm. The sampler's flow rate was adjusted to 200 liter per minute and a quartz filter (diameter 10.2 cm) was used to filter suspended airborne particles. Prior to use, all filters were conditioned for 24 hours in an electric chamber with humidity set at 35 ± 5% and temperature set at 25 ± 5°C prior to both on and off weighing. Filters were placed in sealed plastic compact disc cases during transport and storage process.
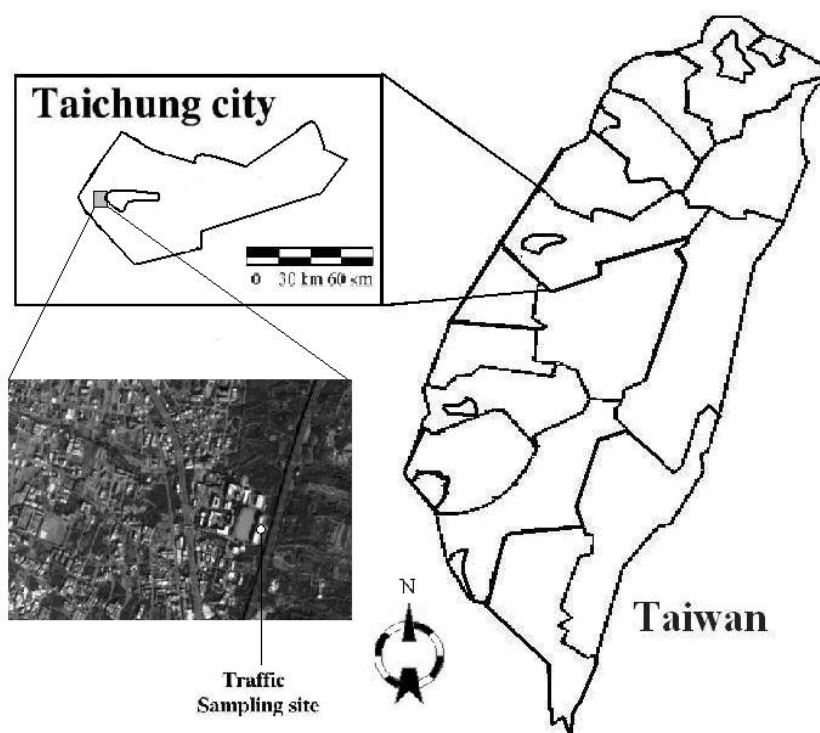
Fig. 1. The location of this highway traffic sampling site in central Taiwan.

Versatile Air Pollutant Sampler

The Versatile air pollutant sampler (VAPS, URG-3000K, URG Corp., Chapel Hill, NC, USA) was utilized to collect $PM_{2.5}$ and $PM_{2.5-10}$ samples simultaneously. Sampling over a 24-h period was performed 6–10 times per month during the two sampling periods. The VAPS sampler has a single inlet assembly (PM_{10}) and is designed to remove particles with aerodynamic diameters > 10. Flow rate is 32 L/min. Quartz filters with a diameter of 47 mm (ZeflourTM Supported PTFE, PALL) were used to collect ambient particulates.

Dry Deposition Plate

The dry deposition plate (DDP) used in this study has a smooth, horizontal, surrogate surface and provides a lower bound estimate of the dry deposition flux. The DDP consisted of a smooth surface plate made of polyvinyl chloride (PVC) that measured 21.5 cm long, 8.0 cm wide and 0.8 cm thick. The DDP also contained a sharp, leading edge that was pointed into the prevailing wind. All filters were maintained in a condition of 50% relative humidity and temperature of 25°C for over 48 h. Prior to sampling use, all filters were weighed to 0.0001 gram-significant digits.

Formula and Calculation

After exposure in the atmosphere for equilibration, the procedures were divided into following steps:
1. Wash the cut surrogate surface (44 cm^2).
2. Coat the adsorbent (silicone grease or apenzon L grease).
3. Weigh filter after moisture equilibrium (24hrs) (W0).
4. Expose the filter in the field and record sampling day and sampling time (t) (24hrs and 48 hrs).

5. Reweigh filter after the moisture equilibrium (W1), and store until Hg analysis.

The following equations were used to determined particle concentration and dry deposition flux:

$$\text{Concentration} = [w1 - w0]/[t(\min) \times Q(\text{liter/min})] \quad (19)$$
$$\text{Flux} = [w1 - w0](ug)/[\text{Area}(m^2) \times t(\min)] \quad (20)$$
$$Vd(\text{cm/sec}) = \text{Flux}(\mu g/m^2\text{-min})/TSP(\mu g/m^3) \quad (21)$$

Chemical Analysis

Concentrations of Hg from each sample (quartz filter, overhead projection film) were analyzed by a direct Hg analyzer (DMA-80 Milestone, Inc., Shelton, CT, USA). Approximately 30 mg of the filter sample was loaded directly into the DMA and analyzed using methods described previously (Basu *et al.*, 2009).

The methodology is based on a thermal decomposition of the sample and collection of the Hg vapor on a gold amalgamator. The filter samples were placed into a sampling boat and transferred to a combustion tube containing a catalyst. The sample is first dried at 200°C prior to combustion at 615–650°C in an oxygen atmosphere. The Hg vapor is collected in a gold amalgamator and after a pre-defined time at 170°C the gold amalgamator is heated up to 900°C. The released Hg is transported to a heated cuvette at 125°C and then analyzed by atomic absorption spectrometry (AAS) using a silicon UV diode detector. The operation conditions were: drying for 30 sec at 200°C, decomposition for 90 sec at 650°C, and combustion for 90 sec at 650°C.

Analytical accuracy and precision were monitored through the use of Standard Reference Materials (SRMs), and intermittent analysis of duplicate samples and blanks.

SRMs included National Research Council of Canada (NRCC) DOLT-3 (dogfish liver) and TORT-2 (lobster hepatopancreas). Average accuracy was within 10% of certified values for all analyses; similarly analytical precision (% Relative Standard Deviation of replicate samples) averaged < 10% for all analyses. All values were back-calculated and presented as an estimated concentration of total Hg on the entire filter.

Quality Control

Analytical accuracy and precision were determined through the use of Standard Reference Materials (DOLT-3 and TORT-2 from National Research Council of Canada) and intermittent analysis of duplicate samples. Average recovery rates of DOLT-3 and TORT-2 for total mercury (Hg) were within the certified values (±10%). The detection limit for the direct Hg analyzer (DMA-80 Milestone, Inc., Shelton, Connecticut, USA) was 0.025 ng and ranged from 0.022 to 0.030 ng.

RESULTS AND DISCUSSION

This sampling information (average temperature, relative humidity, wind speed, and prevailing wind) about ambient air (total, fine and coarse) particulate concentrations are displayed in Table 1. In general, the wind was blowing mainly from the north during March 17 to May 22 of 2009. The average values for temperature, relative humidity and wind speed were 27.0°C, 67.6% and 2.6 m/sec, respectively at this near-highway traffic sampling site. The prevailing wind was blowing directly from the southeast wind during the sampling period in this study.

Table 1 also describes the average total suspended particulate (TSP) concentrations, fine particle ($PM_{2.5}$) and coarse particle ($PM_{2.5-10}$) concentrations at this near highway traffic sampling site during March 17 to May 22 of 2009. The average total suspended particulate concentration was 65.14 $\mu g/m^3$. In addition, the average $PM_{2.5}$ and $PM_{2.5-10}$ concentrations at this near-highway traffic sampling site were 15.47 $\mu g/m^3$ and 9.50 $\mu g/m^3$, respectively. Moreover, the average total suspended particulates concentrations were about 4.21 times as that of fine particulates concentrations and the average fine particulates concentrations were about 1.62 times as that of coarse particulates concentrations at this traffic sampling area.

Table 2 shows the average $PM_{2.5}$, $PM_{2.5-10}$ and PM_{10} concentration by using Versatile Air Pollutant Sampler (VAPS) at the sampling site. The ranges for $PM_{2.5}$, $PM_{2.5-10}$ and PM_{10} particulates were 5.78–29.57 $\mu g/m^3$, 3.89–30.39 $\mu g/m^3$ and 9.67–51.84 $\mu g/m^3$, respectively. The average ratio of fine-to-coarse particulate matter was 1.82 during the sampling period at the sampling site.

Table 1. Meteorological conditions for ambient air total suspended particulates, fine and coarse particulates concentrations at a near high way traffic area during March to May of 2009

Sample No.	Sample date	Temp. (°C)	WS (m/sec)	RH (%)	PWD	Total suspended particulate ($\mu g/m^3$)	$PM_{2.5}$ particulate concentration ($\mu g/m^3$)	$PM_{2.5-10}$ particulate concentration ($\mu g/m^3$)	PM_{10} particulate concentration ($\mu g/m^3$)
1	317	21.7	1.8	62.6	WSS	86.41	25.81	17.86	43.66
2	318	24.7	2.3	63.1	WSS	67.25	29.57	16.62	46.19
3	326	21.9	4.0	73.9	WSW	94.77	21.49	30.39	51.87
4	331	18.8	1.2	62.1	NWW	59.58	15.56	5.65	21.21
5	401	17.7	1.3	61.3	NW	64.81	22.16	7.57	29.73
6	402	18.5	1.5	64.7	NW	68.64	13.75	5.48	19.23
7	403	20.5	0.7	79.6	NW	78.75	23.81	7.75	31.56
8	410	21.4	0.9	76.8	NW	75.26	23.04	10.25	33.30
9	411	22.8	1.2	80.0	WSW	58.54	16.21	12.31	28.53
10	503	25.0	4.0	71.5	NWW	37.98	8.97	7.89	16.86
11	507	25.5	2.7	58.2	WSS	71.43	13.71	9.12	22.80
12	508	25.8	2.2	60.0	WSS	75.26	10.06	10.00	20.06
13	509	25.8	1.7	66.2	WSS	83.28	17.61	9.31	26.92
14	511	27.0	1.7	52.9	SW	53.66	11.38	7.06	18.45
15	512	27.4	2.0	68.6	WSS	33.45	6.34	4.02	10.37
16	513	26.4	4.0	75.1	NW	63.76	10.31	4.84	15.16
17	520	28.1	1.9	77.4	WSS	71.43	5.78	3.89	9.67
18	521	29.5	2.0	71.4	WSS	48.08	7.50	4.06	11.56
19	522	29.6	4.1	74.9	WNW	45.30	10.83	6.51	17.34
Average		27.0	2.6	67.6		65.14	15.47	9.50	24.94
Standard deviation		1.6	1.0	8.2		16.30	7.08	6.38	12.11

Temp: Temperature, WS: Wind speed, RH: Relative Humidity, PWD: Prevailing wind.

Table 3 shows the atmospheric particulates for $PM_{2.5}$, $PM_{2.5}$–PM_{10}, PM_{10} Hg(p) particulates concentrations and ratios for fine/coarse Hg particulate. The ranges of Hg(p) for $PM_{2.5}$ particulates were from 0.0016 to 0.0557 ng/m^3 while the ranges of Hg(p) for $PM_{2.5}$–PM_{10} Hg(p) particulates were from 0.0006 to 0.0305 ng/m^3. And the ratios for fine/coarse Hg(p) particulates were about 1.07. The ranges for PM_{10} Hg(p) particulates concentrations were from 0.0022 to 0.862 ng/m^3.

Table 4 displayed the comparison of various ambient air particle bound pollutants dry deposition velocity during year of 1981–2009. The results indicated that the above mentioned ambient air particle bound pollutants dry deposition velocity were ranged from 0.16 cm/sec to about 5.2 cm/sec in the PCBs. And the ambient air particle bound PAHs pollutants dry deposition velocities were ranged from 4. 5 ± 3.1 to 6.7 ± 2.8 cm/sec. And the average ambient air particle bound PCDD pollutants dry deposition velocities were 0.723 cm/sec. In addition, the average particle bound mercury Hg(p) dry deposition velocity was

Table 2. $PM_{2.5}$, $PM_{2.5}$–PM_{10}, PM_{10}, total suspended particle mass concentrations and their ratios for all the samples collected in this study. $(\mu g/m^3)(N = 19)$

Particulates sizes		Total suspended particulate concentration $(\mu g/m^3)$	$PM_{2.5}$ particulate concentration $(\mu g/m^3)$	$PM_{2.5}$–PM_{10} particle concentration $(\mu g/m^3)$	PM_{10} particulate concentration $(\mu g/m^3)$	Ratios for fine/coarse particulate
Sampling period	Range	33.45–94.77	5.78–29.57	3.89–30.39	9.67–51.87	0.71–3.07
	Mean	65.14	15.47	9.5	24.97	1.82

Table 3. Atmospheric particulates for $PM_{2.5}$, $PM_{2.5}$–PM_{10}, PM_{10} Hg(p) particulates concentrations and Ratios for fine/coarse Hg(p) particulates. $(N = 19)$

Particulates sizes		Total suspended particulate Hg(p) concentration (ng/m^3)	$PM_{2.5}$ Hg(p) concentration (ng/m^3)	$PM_{2.5}$–PM_{10} Hg(p) concentration (ng/m^3)	PM_{10} Hg(p) concentration (ng/m^3)	Ratios for fine/coarse Hg particulate
Sampling period	Range	0.0245–0.1503	0.0016–0.0557	0.0006–0.0305	0.0022–0.862	0.39–2.67
	Mean	0.0763	0.1140	0.0106	0.0220	1.0600

Table 4. Comparison of various ambient air particle bound pollutants dry deposition velocity (cm/sec) during of 1979–2009.

Compounds	Velocity (cm/sec)	Ref
PCB-1242	0.5	Eisenreich *et al*. (1983)
PCB-1016	0.04	Eisenreich *et al*. (1983)
[1]PCB	1.1[c] 5.9[d]	Lee (1991)
[1]PCB	0.723	Lee *et al*. (1996a)
[1]PCB	5	Holsen *et al*. (1991)
PCBs	0.16 ± 0.13	Swackhamer *et al*. (1988)
PCBs	0.5	Doskey and Andren (1981)
PCBs	0.5	Holsen *et al*. (1991)
PCBs	0.18	Atlas *et al*. (1982)
PCBs	1.18	Lee *et al*. (1996b)
PCDD	0.723	Lee *et al*. (2009)
PCBs	5.2	Tasdemir *et al*. (2004)
PCBs	4.2	Tasdemir *et al*. (2005)
PCBs	4.4 ± 7.2	Franz *et al*. (1998)
PCBs	1.26 ± 1.86	Cindoruk and Tasdemir (2007)
[1]PAH	6.7 ± 2.8	Odabasi *et al*. (1999)
[1]PAH	4.5 ± 3.1	Vardar *et al*. (2002)
Hg(p)	3.49 ± 2.0	This study

[1]Greased dry deposition plates, [c]For fine particles, [d]For coarse particles.

3.49 ± 2.0 cm/sec. In general, the average dry deposition velocities order for ambient air particle bound pollutants was PAHs > Hg(p) > PCBs > PCDD.

Fig. 2 displays the particle-bound mercury Hg(p) compositions variations in $PM_{2.5}$, $PM_{2.5-10}$ and TSP. In general, the highest particle-bound mercury Hg(p) compositions in $PM_{2.5}$ were 16.85 ng/g and the lowest particle-bound mercury Hg(p) compositions in $PM_{2.5}$ were 0.55 ng/g. And the highest particle-bound mercury Hg(p) compositions in $PM_{2.5-10}$ were 9.58 ng/g and the lowest particle-bound mercury Hg(p) compositions in $PM_{2.5-10}$ were 0.22 ng/g. Finally, the highest particle-bound mercury Hg(p) compositions in TSP were 77.60 ng/g and the lowest particle-bound mercury Hg(p) compositions in TSP were 15.50 ng/g. The compositions variations for Hg(p) in $PM_{2.5}$, $PM_{2.5-10}$ and TSP are varied. The average compositions

ratios for TSP/Fine and TSP/Coarse were 13.46 and 16.39 for 19 sampling groups in this study, respectively.

Fig. 3 displayed average concentration ratios for TSP/fine and TSP/coarse in particle bound mercury Hg(p) during the 19 sampling groups. The results indicate that the average concentration ratios for TSP/fine and TSP/coarse in particle-bound mercury Hg(p) were 13.46 and 16.40, respectively. In general, the highest concentrations ratios for TSP/fine and TSP/course were 36.38 and 97.01, respectively. The lowest concentrations ratios for TSP/fine and TSP/course were 2.51 and 3.30, respectively.

The average dry deposition mass fluxes were 145.04 $\mu g/m^2$-min. Fig. 4 displays the calculated/measured mass dry deposition flux ratios by Baklanov and Sorensen (2001) and Zhang *et al.* (2001) models for the 19 sampling groups. The results indicate that the average calculated/measured
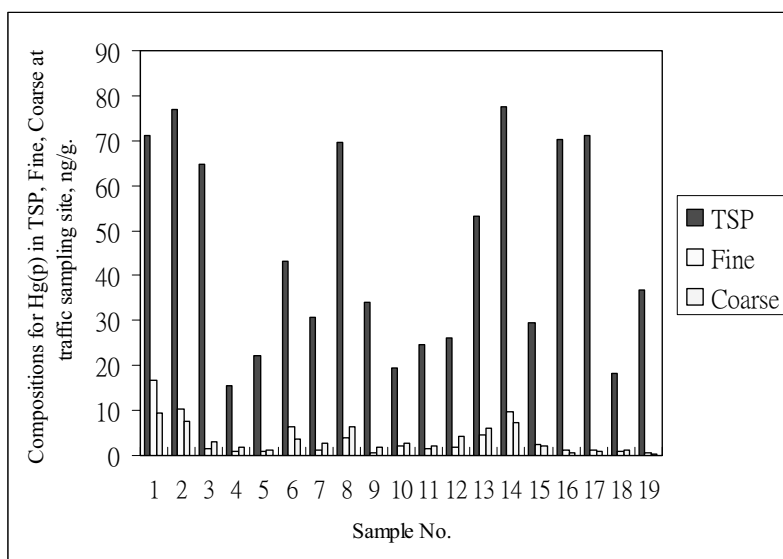

Fig. 2. Average compositions for Hg(p) in TSP, $PM_{2.5}$, $PM_{2.5-10}$ at a traffic sampling site, ng/g.
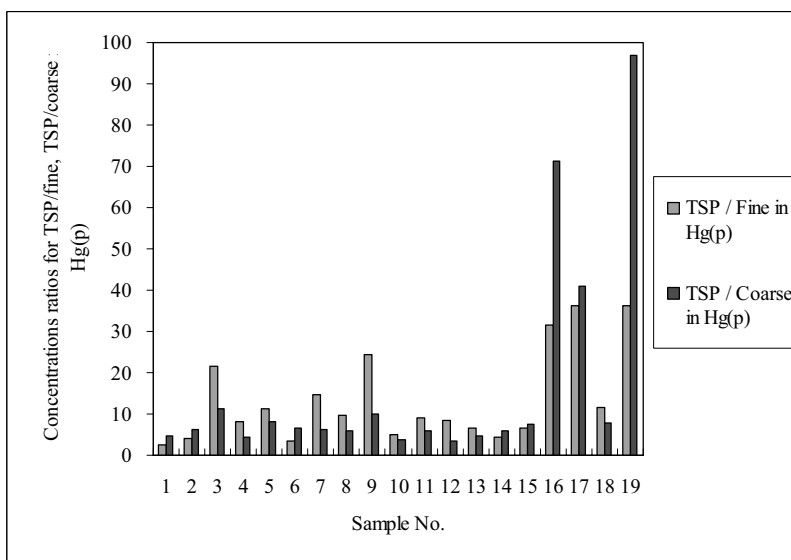

Fig. 3. Average Concentrations ratios for TSP/fine, TSP/coarse in Hg(p) at a traffic sampling site.

mass dry deposition flux ratios value by Baklanov and Sorensen (2001) model was 4.65 while the average calculated/measured mass dry deposition flux ratios values by Zhang *et al*. (2001) was 7.16. Both of these models overestimate the measured dry deposition mass flux. The Baklanov model performed better results in the prediction of mass dry deposition flux.

In addition, the measured dry deposition fluxes for ambient air particulates were ranged from 31.68–380.11 $\mu g/m^2$-min for the 19 sampling groups.

The average dry depositions mass fluxes were 0.95 ng/m^2-min. Fig. 5 displays the calculated/measured mass dry deposition for particle bound Hg(p) flux ratios by Baklanov and Sorensen (2001) and Zhang *et al*. (2001) models for the 19 sampling groups. The results indicate that the average calculated/measured mass dry deposition flux ratios value by Baklanov and Sorensen (2001) model was 0.52 while the average calculated/measured mass dry

deposition flux ratios values by Zhang *et al*. (2001) was 0.81. Both of these two models slightly underestimate the measured dry deposition mass flux for particle bound Hg(p). Zhang's model performed better results in the prediction of Hg(p) dry deposition flux.

In addition, the measured dry deposition Hg(p) fluxes for ambient air particulates were ranged from 0.4218–1.6447 ng/m^2-min for the 19 sampling groups.

CONCLUSIONS

The main conclusions for this study was listed as followed:
1. The average total suspended particulate concentration was 65.14 $\mu g/m^3$. In addition, the average $PM_{2.5}$ and $PM_{2.5-10}$ concentration at this near-highway traffic sampling site were 15.47 $\mu g/m^3$ and 9.50 $\mu g/m^3$, respectively.
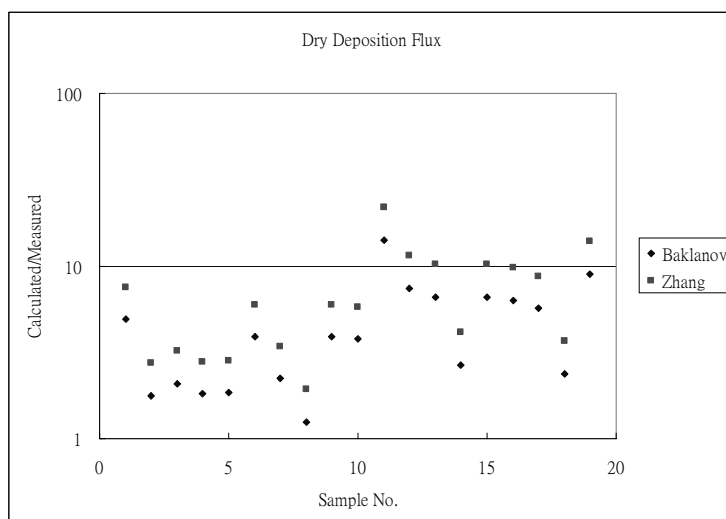

Fig. 4. The average calculated/measured particulates dry deposition flux at a traffic sampling site.
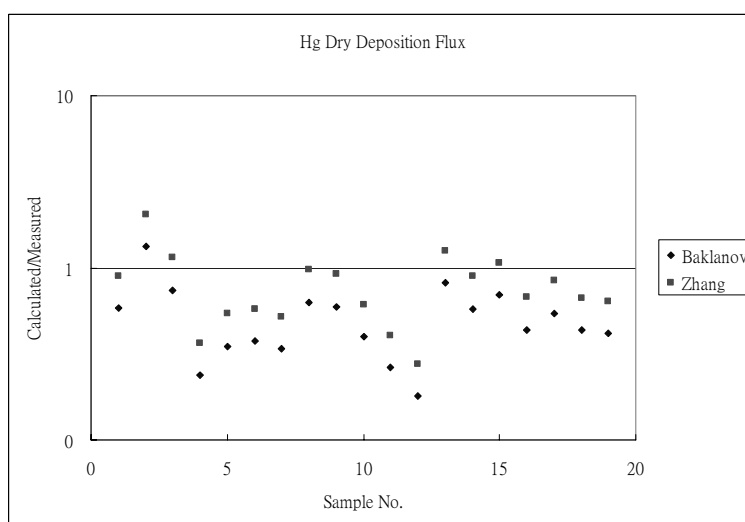

Fig. 5. The average calculated/measured particulates dry deposition flux for particulates bound mercury Hg(p) at a traffic sampling site.

2. The ranges of Hg(p) for PM$_{2.5}$ particulates were from 0.0016 to 0.0557 ng/m^3 while the ranges of Hg(p) for PM$_{2.5}$–PM$_{10}$ Hg(p) particulates were from 0.0006 to 0.0305 ng/m^3. And the ratios for fine/coarse Hg(p) particulates were about 1.07. The ranges for Hg(p) in PM$_{10}$ particulates concentrations were from 0.0022 to 0.862 ng/m^3 .

3. The average composition ratios for TSP/Fine and TSP/Coarse were 13.46 and 16.39 for 19 sampling groups in this study, respectively. The results also indicate that the average concentration ratios for TSP/fine and TSP/coarse in particle bound mercury Hg(p) were 13.46 and 16.40, respectively. In general, the highest concentrations ratios for TSP/fine and TSP/coarse were 36.38 and 97.01, respectively. The lowest concentrations ratios for TSP/fine and TSP/coarse were 2.51 and 3.30, respectively.

4. The average calculated/measured mass dry deposition flux ratios value by Baklanov and Sorensen (2001) model was 4.65 while the average calculated/ measured mass dry deposition flux ratios values by Zhang *et al.* (2001) was 7.16. Both of these two models overestimate the measured dry deposition mass flux. The Baklanov model performed better results in the prediction of mass dry deposition flux.

5. The average calculated/measured mass dry deposition flux ratios value by Baklanov and Sorensen (2001) model was 0.52 while the average calculated/measured mass dry deposition flux ratios values by Zhang *et al*. (2001) was 0.81. Both of these two models slightly underestimate the measured dry deposition mass flux for particle bound Hg(p). Zhang's model performed better results in the prediction of Hg(p) dry deposition flux.

ACKNOWLEDGMENTS

REFERENCES

Atlas, E., Foster, R. and Giam, C.S. (1982). Air-sea Exchange of High-molecular Weight Organic Pollutants: Laboratory Studies. *Environ. Sci. Technol.* 16: 283–286.

Baklanov, A. and Sorensen, J.H. (2001). Parameterisation of Radionuclide Deposition in Atmosphere Long-range Transport Modeling. *Phys. Chem. Earth*. 26: 787–799.

Basu, N., Scheuhammer, A.M., Sonne, C., Letcher, R.J., Born, E.W. and Dietz, R. (2009). Is Dietary Mercury of Neurotoxicological Concern to Wild Polar Bears (Ursus Maritimus)? *Environ. Toxicol. Chem.* 28: 133-140.

Bullock, O.R. (2000). Modeling Assessment of Transport and Deposition Patterns of Anthropogenic Mercury Air Emissions in the United States and Canada. *Sci. Total Environ.* 259: 145–157.

Bullock, O.R. and Brehme, K.A. (2002). Atmospheric Mercury Simulation Using the CMAQ Model: Formulation Description and Analysis of Wet Deposition Results. *Atmos. Environ.* 26: 2135–2146.

Calvert, J.G. and Lidberg, S.E. (2005). Mechanisms of Mercury Removal by O$_3$ and OH in the Atmosphere. *Atmos. Environ.* 39: 3355–3367.

Cindoruk, S.S. and Tasdemir, Y. (2007). Deposition of Atmospheric Particulate PCBs in Suburban Site of Turkey. *Atmos. Res.* 85: 300–309.

Cohen, M., Artz, R., Draxler, R., Miller, P., Poissant, L., Niemi, D., Ratte, D., Deslauriers, M., Duval, R., Laurin, R., Slotnick, J., Nettesheim, T. and McDonald, J. (2004). Modeling the Atmospheric Transport and Deposition of Mercury to the Great Lakes. *Environ. Res.* 95: 247–265.

Dastoor, A. and Larocque, Y. (2004). Global Circulation of Atmospheric Mercury: A Modeling Study. *Atmos. Environ.* 38: 147–161.

Doskey, P.V. and Andren, A.W. (1981). Modeling the Flux of Atmospheric Polychlorinated Biphenyls across the Air/Water Interface. *Environ. Sci. Technol.* 15: 705–711.

Dvonch, J.T., Graney, J.R., Marsik, F.J., Keeler, G.J. and Stevens, R.K. (1998). An Investigation of Source–Receptor Relationships for Mercury in South Florida Using Event Precipitation Data. *Sci. Total Environ.* 213: 65–108.

Eisenreich, S.J., Looney, B.B. and Hollod, G.J. (1983). In *Physical Behavior of PCBs in the Great Lakes*, Mackay, D., Paterson, S., Eisenreich, S.J. and Simmons, M.S. (Eds.), Ann Arbor Science, Ann Arbor, MI, United States, p. 115–125.

Engle, M. and Gustin, M.S. (2002). Scaling of Atmospheric Mercury Emissions from Three Nnaturally Enriched Areas: Flowery Peak, Nevada; Peavine Peak, Nevada; And Long Valley Caldera, California. *Sci. Total Environ.* 290: 91–104.

Engle, M., Gustin, M.S. and Zhang, H. (2001). Quantifying Natural Source Mercury Emissions from the Ivanhoe Mining District, North-central Nevada, USA. *Atmos. Environ.* 35: 3987–3997.

EPRI (1996). Mercury in the Environment FA Research Update. EPRI Report No. TR-107695, 3081, 3508, 329, Electric Power Research Institute, Palo Alto, California.

Fang, G.C., Wu, Y.S., Huang, S.H. and Ran, J.Y. (2006). Size Distributions of Ambient Air Particles and Enrichment Fa In *Handbook of Applied Meteorology* ctor Analyses of Metallic Elements at Taichung Harbor near the Taiwan Strait. *Atmos. Res*. 81: 320–333.

Franz, T.P., Eisenreich, S.J. and Holsen, T.M. (1998). Dry Deposition of Particulate Polychlorinated Biphenyls and Polycyclic Hydrocarbons to Lake Michigan. *Environ. Sci. Technol.* 32: 3681–3688.

Gbor, P.K., Wen, D., Meng, F., Yang, F., Zhang, B. and Sloan, J. (2006). Improved Mercury Model for Mercury Emission, Transport and Deposition. *Atmos. Environ.* 40: 973–983.

Ghose, M. and Majee, S. (2007). Characteristics of Hazardous Airborne Dust around an Indian Surface Coal Mining Area. *Environ. Monit. Assess.* 130: 17–25

Giorgi, F. (1988). Dry Deposition Velocities of Atmospheric

Aerosols as Inferred by Applying a Particle Dry Deposition Parameterization to a General Circulation Model. *Tellus Ser. B* 40: 23–41.

Gong, S.L., Barrie, L.A., Blanchet, J.P., von Salzen, K. Lohmann, U., Lesins, G., Lavoue, D.H., Jiang, J., Lin, H., Girard, E., Leaitch, R., Leighton, H., Chylek, P. and Spacek, L. (2000). CAM: Treatment of the Size Segregated Atmospheric Aerosols for Climate and Air Quality Models. Part 1. Module Development. *J. Geophys. Res.* submitted for publication.

Gustin, M.S., Lindberg, S., Marsik, F., Casimir, A., Ebinghaus, R., Edwards, G., Hubble-Fitzgerald, C., Kempt, R., Kock, H., Leonard, T., London, J., Majewski, M., Montecinos, C., Owens, J., Pilote, M., Poissant, L., Rasmussen, P., Schaedlich, F., Schneeberger, D., Schroeder, W., Sommar, J., Turner, R., Vette, A., Wallschlaeger, D., Xiao, Z. and Zhang, H. (1999). Nevada STORMS Project: Measurement of Mercury Emissions from Naturally Enriched Surfaces. *J. Geophys. Res.* 104: 21831–21844.

Han, Y.J., Holsen, T.M. and Hopke, P.K. (2007). Estimation of Source Locations of Total Gaseous Mercury Measured in New York State Using Trajectory-Based Models. *Atmos. Environ.* 41: 6033–6047.

Hinds, W.C. (1982). *Aerosol Technology.* Wiley, New York, p. 38–68 and 211–232.

Holsen, T.M., Noll, K.E., Liu, S. and Lee, W. (1991). Dry Deposition of Polychlorinated Biphenyls in Urban Areas. *Environ. Sci. Technol.* 25: 1075–1081.

Lee, W.J. (1991). The Determination of Dry Deposition Velocities for Gases and Particles. Ph.D. Thesis, Illinois Institute of Technology.

Lee, W.J., Lewis Lin, S.J., Chen, Y.Y., Wang, Y.F., Sheu, H.L., Su, C.C. and Fan, Y.C., (1996b). Polychlorinated Biphenyls in the Ambient Air of Petroleum Refinery, Urban and Rural Areas. *Atmos. Environ.* 30: 2371–2378.

Lee, W.J., Shih, S.I., Li, H.W., Lin, L.F., Yu, K.M., Lu, K., Wang, L.C., Chang-Chien, G.P., Fang, K., Lin, M., (2009). Assessment of Polychlorinated Dibenzo-*p*-dioxins and Dibenzofurans Contribution from Different Media to Surrounding Duck Farms. *J. Hazard. Mater.* 163: 1185–1193.

Lee, W.J., Su, C.C., Sheu, H.L., Fan, Y.C., Chao, H.R. and Fang, G.C. (1996a). Monitoring and Modeling of PCB Dry Deposition in Urban Area. *J. Hazard. Mater.* 49: 57–88.

Lin, C., Cheng, M. and Schroeder, W. (2001). Transport Patterns and Potential Sources of Total Gaseous Mercury Measured in Canadian High Arctic in 1995. *Atmos. Environ.* 35: 1141–1154.

Lin, C.J. and Pehkonen, S.O. (1999).The Chemistry of Atmospheric Mercury: A Review. *Atmos. Environ.* 33: 2067–2079.

Lindberg, S.E., Zhang, H., Vette, A.F., Gustin, M.S., Barnette, M.O. and Kuiken, T. (2002). Dynamic Flux Chamber Measurement of Gaseous Mercury Emission Fluxes over Soils. Part 2–Effect of Flushing Flow Rate and Verification of a Two-resistance Exchange Interface Simulation Model. *Atmos. Environ.* 36: 847–859.

Liu, B., Keeler, G.J., Dvonch, J.T., Barres, J.A., Lynam, M.M., Marsik, F.J. and Morgan, J.T. (2007). Temporal Variability of Mercury Speciation in Urban Air. *Atmos. Environ.* 41: 1911–1923.

Näslund, E. and Thaning, L. (1991). On the Settling Velocity in a Nonstationary Atmosphere. *Aerosol Sci. Technol.* 12: 247–256.

Odabasi, M., Sofuoglu, A., Vardar, N., Tasdemir, Y. and Holsen, T.M. (1999). Measurement of Dry Deposition and Air–water Exchange of Polycyclic Aromatic Hydrocarbons with the Water Surface Sampler. *Environ. Sci. Technol.* 33: 426–434.

Pai, P., Karamchandani, P. and Seigneur, C. (1997). Simulation of the Regional Atmospheric Transport and Fate of Mercury Using a Comprehensive Eulerian Model. *Atmos. Environ.* 31: 2717–2732.

Petersen, G., Bloxam, R., Wong, S., Munthe, J., Kruger, O., Schmolke, S.R. and Kumar, A.V. (2001). A Comprehensive Eulerian Modeling Framework for Airborne Mercury Species: Model Development and Applications in Europe. *Atmos. Environ.* 35: 3063–3074.

Poissant, L. (1999). Potential Sources of Atmospheric Total Gaseous Mercury in the St. Lawrence River Valley. *Atmos. Environ.* 33: 2537–2547.

Ruijgrok, W., Davidson, C.I. and Nicholson, K.W. (1995). Dry Deposition of Particles - Implications and Recommendations for Mapping of Deposition over Europe. *Tellus Ser. B* 47: 587–601.

Ryaboshapko, A., Bullock, R., Ebinghaus, R., Ilyin, I., Lohman, K., Munthe, J., Petersen, G., Seigneur, C. and Wangberg, I. (2002). Comparison of Mercury Chemistry Models. *Atmos. Environ.* 36: 3881–3898.

Sakata, M. and Asakura, K. (2007). Estimating Contribution of Precipitation Scavenging of Atmospheric Particulate Mercury to Mercury Wet Deposition in Japan. *Atmos. Environ.* 41: 1669–1680.

Schroeder, W.H. and Munthe, J. (1998). Atmospheric Mercury Fan Overview. *Atmos. Environ.* 32: 809–822.

Seigneur, C., Karamchandani, P., Lohman, K., Vijayaraghavan, K. and Shia, R.L. (2001). Multiscale Modeling of the Atmospheric Fate and Transport of Mercury. *J. Geophys. Res.* 106: 27795–27809.

Shannon, J.D. and Voldner, E.C. (1995). Modeling Atmospheric Concentrations of Mercury and Deposition to the Great Lakes. *Atmos. Environ.* 29: 1649–1661.

Slinn, W.G.N. (1982). Predictions for Particle Deposition to Vegetative Canopies. *Atmos. Environ.* 16: 1785–1794.

Swackhamer, D.L., McVeety, B.D. and Hites, R.A. (1988). Deposition and Evaporation of Polychlorobiphenyl Congeners to and from Siskiwit Lake, Isle Royale, Lake Superior. *Environ. Sci. Technol.* 22: 664–672.

Tasdemir, Y., Odabasi, M. and Holsen, T.M. (2005). Measurement of the Vapor Phase Deposition of Polychlorinated Biphenyls (PCBs) Using a Water Surface Sampler. *Atmos. Environ.* 39: 885–897.

Tasdemir, Y., Odabasi, M., Vardar, N., Sofuoglu, S., Murphy, T.J. and Holsen, T.M. (2004). Dry Deposition Fluxes and Velocities of Polychlorinated Biphenyls (PCBs) Associated with Particles. *Atmos. Environ.* 38:

2447–2456.

Travnikov, O. (2005). Contribution of the Intercontinental Atmospheric Transport to Mercury Pollution in the Northern Hemisphere. *Atmos. Environ.* 39: 7541–7548.

United Sates Environmental Protection Agency (USEPA) (1998). Mercury Study Report to Congress, EPA-452/R-97-0003, USEPA Office of Air Planning and Standards, Office of Research and Development.

Vardar, N., Odabasi, M. and Holsen, T.M. (2002). Particulate Dry Deposition and Overall Deposition Velocities of Polycyclic Aromatic Hydrocarbons. *J. Environ. Eng.* 128: 269–274.

Wallschlager, D., Turner, R.R., London, R., Kock, H.H., Sommar, J. and Xioa, Z. (1999). Factors Affecting the Measurement of Mercury Emissions from Soils with Flux Chambers. *J. Geophys. Res.* 104: 21859–21871.

Wesely, M.L. (1989). Parameterisation of Surface Resistances to Gaseous Dry Deposition in Regional Scale Numerical Models. *Atmos. Environ.* 23: 1293–1304.

Yamartino, R.J. (1989). In *Handbook of Applied Meteorology,* Atmospheric Pollutant Deposition Modeling. Chapter 27. Houghton, D.D. (Ed.), A Wiley-Interscience Publication, New York. p. 754–766.

Zannetti, P. (1990). *Air Pollution Modeling, Theories, Computational Methods and Available Software*, Computational Mechanics, Southampton and Van Nostrand Reinhold, New York.

Zhang, H., Lindberg, S.E., Barnette, M.O., Vette, A.F. and Gustin, M.S. (2002). Dynamic Flux Chamber Measurement of Gaseous Mercury Emission Fluxes over Soils. Part 1: Simulation of Gaseous Mercury Emissions from Soils Using a Two-resistance Exchange Interface Model. *Atmos. Environ.* 36: 835–846.

Zhang, L., Gong, S., Padro, J. and Barrie, L. (2001). A Size-segregated Particle Dry Deposition Scheme for an Atmospheric Aerosol Module. *Atmos. Environ.* 35: 549–560.